A two-step biosorption methodology for efficient and rapid removal of Fe(II) following As(V) from aqueous solution using abundant biomaterials

Kenza Richards, Armelle Garcia, Yves-Marie Legrand, Claude Grison

A two-step biosorption methodology for efficient and rapid removal of Fe(II) following As(V) from aqueous solution using abundant biomaterials

K. Richards[1] · A. Garçia[1] · Y.- M. Legrand[1] · C. Grison[1]

Abstract
An innovative methodology was implemented for removing arsenic from aqueous solution by developing successive biosorption experiments. Considering the high affinity of As oxyanions toward Fe(III) oxides, the biosorption of Fe(II) was first conducted using nine biomaterials—aquatic and terrestrial invasive species, biowastes, local plants. *Pistia stratiotes*, an invasive alien species presenting the highest concentration of adsorbed Fe(II), was selected for a detailed investigation of As(V) removal from wastewater. After oxidation of the biosorbent into Fe(III), it yielded to a 92% removal efficiency determined by GFAAS and an excellent maximum biosorption capacity of 5.1 $mg.g^{-1}$. The biosorbent was characterized by MP-AES and HRTEM-EDX. The adsorption mechanisms for iron and arsenic have been studied via theoretical models and the Langmuir isotherms and pseudo-second-order kinetics models revealed excellent linearity and highlighted the robustness of the method. These promising results were developed to build a pilot for As(V) removal from the Russec river (Orbiel Valley, France), polluted with arsenic.

Keywords Metallic elements · Adsorption · Biosorbents · Invasive alien species · Wastewater treatment

Introduction

Water, sometimes qualified as blue gold, is a vital resource and a precious common good, whose preservation must be a global top priority. Its access and security is suffering from a crisis as severe as the climate crisis (United Nations World Water Development Report: 2021 Valuing Water 2021). Increasingly rare, water is also increasingly polluted and nowadays 80% of polluted waters are discharged in the environment without treatment. Many sources of pollution, organic and inorganic, affect water, and its contamination by heavy metals is one of the most important hazards to water resources.

Arsenic, which is the twentieth most abundant element on the earth's crust, is a toxic metalloid considered as a major worldwide water contaminant (Williams 2001). Three hundred million people residing in more than 100 countries have already been directly or indirectly affected by As toxicity. Arsenic exposure causes damage to the central nervous system and is responsible for the development of liver, bladder, skin and kidney cancers and many other diseases (Monrad et al. 2017). Due to its very high toxicity, the World Health Organization declared a guideline threshold of 10 $\mu g.L^{-1}$ for arsenic in drinking water replacing the old standard of 50 $\mu g.L^{-1}$.

Arsenic decontamination is a hot topic and has been extensively studied. Over the years, various physicochemical and biological methods have been reported. These technologies include coagulation–flocculation, membrane filtration, ion exchange and electrochemical methods (Ghosh et al. 2019). However, these methods involve high-energy input and complicated procedures, making them costly and less attractive to industrialize. Adsorption has recently emerged as an efficient technique for the removal of arsenic, as it is highly efficient, cost-effective, sludge-free and technologically simple (Mohan and Pittman 2007) but remains very new and uncommonly applied in industry (Irshad et al. 2021). Different adsorbents have been intensively

investigated, and iron-enriched adsorbents are largely developed considering the strong natural affinity of iron oxides toward arsenic oxyanions, the environmental friendliness of iron and its abundance on earth (Carlson et al. 2002).

However, major drawbacks have arisen in terms of the cost and low-efficiency of the adsorbent used in common adsorption. In this regard, biosorption has gained popularity due to its low cost, eco-friendliness and abundant availability of the biosorbents. Modified jute fibers (Hao et al. 2015), wheat straw (Tian et al. 2011), oyster shell (Fan et al. 2015), sawdust (Setyono and Valiyaveettil 2014), cork granulates (Pintor et al. 2018), bagasse (Gupta et al. 2015; Pehlivan et al. 2013), waste plant material (Arshad and Imran 2020) and rice bran (Hu et al. 2010) have been reported to enhance the capabilities of arsenic removal using an iron-enriched biomaterial.

In this article, a bio-inspired procedure for removing arsenic oxyanions ($As_xO_y^{m-}$) from effluents is presented. The methodology is based on a two-step biosorption—the biosorption of arsenic using bio-wastes was firstly enriched with iron by a previous biosorption. The study was limited to As(V), which is the most abundant form of arsenic in water as As(III) is rapidly oxidized into As(V) and to the Fe(II) adsorptions, since Fe(II) is the most abundant form of iron in water and Fe(III) is known to poorly adsorb (Sarkar and Paul 2016). We first investigated the biosorption capacity of nine biomaterials toward Fe(II). The most efficient iron biosorbent, *Pistia stratiotes*, was selected to then study the removal of As(V), as it showed the highest concentration of iron. The biosorbents were characterized by GF-AAS and HRTEM-EDX. The adsorption mechanisms for Fe(II) and As(V) were determined by studying their thermodynamics and kinetics, allowing a mathematical modeling. And finally, these studies carried out at a laboratory scale lead to the development of a pilot-scale project for As(V) removal from wastewater *in natura*, in the Russec river (Orbiel Valley, France).

Materials and methods

All chemicals (iron sulfate $FeSO_4 \bullet 7H_2O$ and sodium arsenate $Na_2HAsO_4 \bullet 7H_2O$) were of analytical grade and were purchased from Sigma-Aldrich. The solutions were prepared by dilution with deionized water at neutral pH to stay close to the pH mostly found in nature.

Biomaterials and their preparation

Nine different natural materials, *Pistia stratiotes*, *Ludwigia peploides*, *Mentha aquatica*, *Eichhornia crassipes*, *Fallopia japonica*, wheat straw, pinecone, sawdust and coffee grounds, were considered in order to compare their performances for iron and then arsenic removal from water. Their origin is given in more detail in Online Resource (paragraph 1.1). They were either obtained from a specialized grower (Nymphaea Distribution, Le Cailar, France) or collected from various sites in the Occitanie region of France.

Biomaterial for iron biosorption

Pistia stratiotes, *Ludwigia peploides*, *Mentha aquatica* and *Eichhornia crassipes*, wheat straw, sawdust and pinecones were dried naturally after collection (sun and wind). They were ground with a cutting mill Fritsch pulverisette 19 apparatus at 1 mm, sifted through a 0.5-mm sieves and washed with water (3×100 mL.g^{-1}). They were then dried at 80 °C until stable weight (18 h) before they could be used for biosorption.

Coffee grounds were washed several times with hot water until the filtrate became colorless and then were dried 18 h at 80 °C before biosorption.

Biomaterial for arsenic biosorption

After the preparation of the biomaterial ("Biomaterial for iron biosorption"), an iron biosorption is performed. At the end of the biosorption, the biomaterial is filtered and dried at 80 °C overnight. Then, a thermal treatment is carried out before the biomaterial could be used for arsenic biosorption. From room temperature, the oven is reaching the aimed temperature at maximum rate (150 °C.h^{-1}), then heating for 4 h, natural decrease of temperature to room temperature. The different temperatures studied are 150 °C, 300 °C and 550 °C.

Biosorption experiments

Ferrous manganese aqueous solutions were prepared using the adequate amount of $FeSO_4 \bullet 7H_2O$ dissolved in deionized water to reach the desired concentration.

Arsenate aqueous solutions were prepared from dilution of a 1 $g.L^{-1}$ stock solution made out of sodium arsenate $Na_2HAsO_4 \bullet 7H_2O$ in deionized water.

Each biosorption experiment was conducted in triplicate.

Batch mode

One gram of biomaterial was used per litter of aqueous solution at different initial concentrations, neutral pH and room temperature. The solution was vigorously stirred for 2 h; then, the biomaterials were filtered and dried in an oven at 80 °C until constant weight.

Column mode

One hundred milligrams of biomaterial was loaded in the 250 × 4 mm HPLC column. Then, 100 mL of a solution at different initial concentrations, neutral pH and room temperature was passed through the column at a rate of 4 $mL.min^{-1}$. The solid was then removed from the column and dried at 80 °C until constant weight. The exact concentrations of arsenic solutions before and after biosorption were determined with ICP-MS or FG-AAS analyses. The experiments were performed three times, and the samples were injected in triplicates. RSD (relative standard deviation) is indicated.

Adsorption isotherm

The effects of concentration of Fe(II) or As(V) were analyzed and fitted to the Langmuir and Freundlich models; two common models are used to interpret the experimental result (Choudhary and Bhattacharyya 2020). The Langmuir model represents monolayer adsorption through homogeneous adsorption sites, whereas in terms of the Freundlich model, the adsorption sites are heterogeneous and the adsorption multilayered. More details concerning these two models, mathematical formulas, linearization and fitting with experimental data, are given in supplementary information (SI 1.2.). Solutions of $FeSO_4 \bullet 7H_2O$ (from 5 to 40 $mg.L^{-1}$) and $Na_2HAsO_4 \bullet 7H_2O$ (from 0.05 to 20 $mg.L^{-1}$) were stirred for 2 h with 1 $g.L^{-1}$ of *P. stratiotes* at neutral pH and at 293 K.

Adsorption kinetics

To study the adsorption kinetics, biosorptions of Fe(II) and As(V) have been performed for different durations: from 2 min to 4 h, at different initial concentrations (8 and 40 $mg.L^{-1}$ of $FeSO_4 \bullet 7H_2O$ and 0.05 and 0.5 $mg.L^{-1}$ of $Na_2HAsO_4 \bullet 7H_2O$). Kinetics modeling allows the estimation of sorption rates but also helps understanding the adsorption mechanisms. It is important to be able to predict the rate at which pollutant is removed from aqueous solutions in order to design optimal sorption treatment plants. The experimental data were analyzed according to the pseudo-first- and pseudo-second-order kinetics models, the most commonly used models (SI 1.3.) (Ho and McKay 1999).

Pilot study of biosorption on site

Decontamination of arsenic *in natura* in the Russec River (Domaine du Salitis, Vallée de l'Orbiel, Aude, France) has been investigated at a pilot scale. The mobile pilot was brought close to the Russec River, and the pump plunged into the water. One hundred grams of biosorbent (equivalent to 1.11 $g.L^{-1}$ of adsorbent) was loaded into one adsorption column. The column was then fixed onto the system, and the pump was turned on to fill the input tank. The water was passed through the column at 30 $L.h^{-1}$, and the experiment was performed during 3 h. Samples were collected every 10 min and analyzed by GF-AAS once returned to the laboratory.

Analytical methods

Mineral compositions of aqueous solution and biomaterials before and after biosorption were determined either by microwave plasma-atomic emission spectroscopy (MP-AES), inductively coupled plasma-mass spectrometry (ICP-MS) analyses or graphite furnace atomic absorption spectrometry (GF-AAS).

Digestions of the biomaterials were performed by microwave-assisted dissolution using a Multiwave GO microwave system (Anton Paar®). In this procedure, an exact mass (10 mg) was suspended into a Teflon reactor with a mixture of aq. HCl 37% / aq. HNO_3 65% (2:4, v/v, 6 mL). The reactors were heated according to the following program: rise in temperature from 25 to 165 °C

(20 min), followed by a stage at 165 °C (10 min). After cooling for 30 min, the digests were filtered and then diluted to 0.4 $mg.L^{-1}$ in deionized water.

For the iron study, mineral compositions of aqueous solution and digested materials were determined using a MP-AES 4200 (Agilent Technologies) equipped with a concentric nebulizer and a double-pass cyclonic spray chamber. The arsenic concentrations were determined by ICP-MS performed on a Thermo scientific X Series II ICP-MS (AETE Platform-Hydrosciences, Montpellier-France) or GF-AAS analyses using a Thermo Scientific™ iCE 3300 AAS GF. The analyses were repeated three times.

Iron and arsenic association has been proven by scanning transmission electron microscopy and energy-dispersive X-ray spectroscopy analysis (HRTEM/EDX). The analyses were proceeded on a JEOL 2200 FS operated at 200 kV (MEA Platform—University of Montpellier—France). The images were obtained on a CCD GATAN UltraScan 4092 × 4092 px2, and the chemical composition was assessed via STEM-EDX using a 100-mm^2 windowless Oxford Instruments Xmax TLE detector.

Transmission Mössbauer spectra were recorded by a conventional Mössbauer spectrometer (Wissel) with a flowing gas (96% He, 4% CH_4) proportional counter (Rikon-5) at room temperature. The velocity scale was calibrated with a 57CoRh source and a metallic iron foil.

IR spectra were recorded on a Perkin-Elmer Spectrum 100 FTIR spectrometer in ATR (Attenuated Total Reflexion) mode. The number of scans was 32; the resolution was 1 $point.cm^{-1}$. The acquisition was done from 650 to 4000 cm^{-1}. The detector used was a DTGS (Deuterated-TriGlycine Sulfate). The background was done in air.

Results and discussion

Biosorption of Fe(II)

The biosorption performances of nine biomaterials, with different chemical properties, were investigated for removing Fe(II) from aqueous solutions of iron sulfate. These different biomaterials were chosen since they derive from aquatic, semi-aquatic and terrestrial invasive alien species, bio-wastes and indigene plants, and are hence natural, abundant and priceless.

They were previously characterized by FTIR (Stanovych et al. 2019), allowing their classification in three groups:

Table 1 Langmuir and Freundlich parameters for adsorption of Fe(II) onto nine different biomaterials (1 g)

Isotherm	Param	Biosorbents: 9 different natural materials								
		Group 1		Group 1/2			Group 2		Group 3	
		P. stratiotes	M. aquatica	L. peploides	E. crassipes	F. japonica	Straw	Sawdust	Pine cones	Coffee grounds
Freundlich	R^2	0.7304	0.962	0.939	0.957	0.973	0.913	0.947	0.888	0.980
	K_f ($mg.g^{-1}$)	18.16	3.43	5.05	4.57	2.02	2.50	1.85	1.92	3.89
	n	3.31	1.65	2.39	2.63	2.60	6.05	4.84	9.15	6.15
Langmuir	R^2	0.993	0.998	0.995	0.998	0.999	0.999	0.991	0.958	0.972
	q_m ($mg.g^{-1}$)	59.17	26.81	20.16	15.80	8.47	4.46	3.70	2.86	6.55
	K_L ($L.mg^{-1}$)	0.59	0.11	0.21	0.31	0.19	0.66	0.61	1.13	0.94
	R_L	0.04–0.25	0.18–0.64	0.10–0.48	0.08–0.39	0.12–0.52	0.04–0.23	0.04–0.25	0.02–0.15	0.03–0.18
Experimental*	q_e ($mg.g^{-1}$)	58.07	16.70	15.74	12.50	7.18	4.37	3.41	2.78	6.93

*initial concentration of iron sulfate was 1.2 g/L

(A)

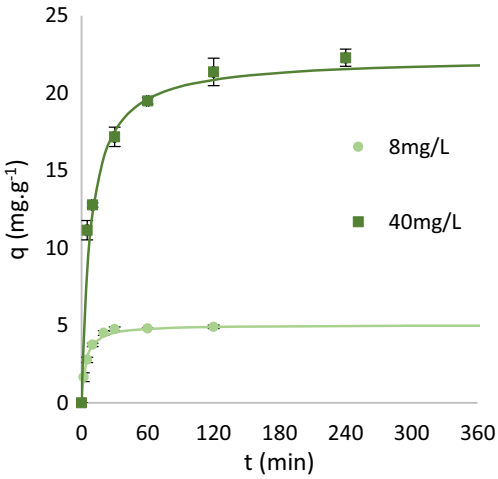

(B)

Kinetics	Parameters	Fe(II) (40 ppm)	Fe(II) (8 ppm)
Pseudo first order	k1 (min-1)	0.055	0.155
	R^2	0.940	0.848
	qe (exp) (mg.g-1)	22.3	4.9
	qe (plot) (mg.g-1)	22.3	4.8
	% deviation	0. 047	1.9
Pseudo second order	k2 (g.mg-1.min-1)	0.005	0.064
	R^2	0.9995	0.9996
	qe (exp) (mg.g-1)	22.3	4.9
	qe (plot) (mg.g-1)	21.9	4.9
	% deviation	1.61	0.16

Fig. 1 **A** Kinetic experimental data and **B** parameters for biosorption of Fe(II) onto *P. stratiotes* for a pseudo-second-order fitting (initial concentrations: 8 and 40 mg.L.$^{-1}$)

- Group 1: carboxylate-rich material (*Pistia stratiotes*, *Ludwigia peploides*, *Mentha aquatica*, *Eichhornia crassipes*, *Fallopia japonica*). These natural materials correspond to aquatic living plants.
- Group 2: lignin-rich material (wheat straw, pine cone, sawdust, *Fallopia japonica*), corresponding to terrestrial biomasses.
- Group 3: tannin-rich material (used coffee grounds).

Fallopia japonica can be classified in between groups 1 and 2, as it is a semi-aquatic plant also having an intermediate chemical composition.

Adsorption isotherms of Fe(II)

The adsorption isotherm experiments of Fe(II) were conducted in batch mode by preparing solutions of iron sulfate with a concentration range of 5–40 mg.L^{-1} and using 1 g of each biosorbent per liter of solution. Experimental equilibrium data were fitted to the Langmuir and Freundlich adsorption isotherm models (Table 1, Online Resource Figs. 2–10).

According to the correlation coefficient (R^2), the Freundlich model fits for most of the biosorbents. The value of the reciprocal Freundlich intensity (1/n) is under 1, reflecting a favorable adsorption onto the surface of the different materials. Yet, the Langmuir model had the best-fitting isotherm for every biosorbent, with very high correlation value (> 0.99 for 7 out of 9 biomaterials). Since following a Langmuir model, these biomaterials provided homogeneous adsorption sites for Fe(II) which adsorbed in a single layer. The Langmuir separation factors R_L were found to be between 0 and 1, indicating that the uptake of Fe(II) is favorable for every material.

Theoretical maximum biosorption capacity (q_m, mg.g^{-1}) was also calculated for each biomaterial, using the Langmuir model since it remarkably fitted with the experimental data. For the nine biomaterials, the maximum adsorption capacities were also confirmed experimentally (Table 1). The best adsorption was accomplished with *P. stratiotes*, which gave a very high maximum biosorption capacity of 59.17 mg.g^{-1} theoretically and 58.07 mg.g^{-1} experimentally using a high concentration of 1.2 g.L^{-1} of iron sulfate. Group 1 of biomaterials showed the best performances, with high maximum adsorption capacity (from 15.74 mg.g^{-1} to 58.07 mg.g^{-1}), followed by the intermediate *F. japonica* (group 1–2) and coffee grounds (group 3).

Groups 1, 1–2 and 3 are good candidates for the removal of iron from wastewater. Finally, group 2 biomaterials have lower performances. It is interesting to note that carboxylate-rich materials (group 1) (Stanovych et al. 2019) have the best performances, which is an important clue regarding the adsorption mechanism suggesting the adsorption of iron by carboxylate moieties.

Adsorption kinetics of Fe(II) onto *P. stratiotes*

Since *P. stratiotes* showed the highest maximum adsorption capacity, this biomaterial was used for kinetics studies (Fig. 1). Two aqueous solutions of iron sulfate (8 and 40 mg.L^{-1}) using 1 g of *P. stratiotes* per liter of Fe(II) solution were used to determine the time required for a maximum adsorption. These initial concentrations were, respectively, chosen to reproduce a usual composition of a mining effluent and to reach a high biosorption capacity calculated by the Langmuir model. Experiments were conducted in batch mode, in triplicate for different timings, from 2 to 240 min. In the case of the low iron concentration (8 mg.L^{-1}), only 30 min are required to adsorb all the ferrous cations in solution and reach the equilibrium. With the highest concentration (40 mg.L^{-1}), the equilibrium is reached later, but still rather quickly as after 60 min, 87% of the iron has been absorbed. The process seemed to be a one step process. A remarkably fast biosorption at the beginning corresponded to rapid filling of the adsorption sites on the surface, reaching the equilibrium where no more adsorption seems to appear from increasing contact time. This equilibrium probably represents a saturation of the adsorption sites. The potentials remaining unsaturated sites could no longer be approached due to repulsion of iron ions in the solid phase with each other and with those in the solution. It is important to point out that no desorption was observed in either case.

These results were analyzed according to the pseudo-first-order and pseudo-second-order models to help elucidate the potential rate-limiting steps of biosorption. Their linearization and experimental fitting are shown in Online Resource Fig. 11, and the characteristic parameters and correlation coefficients are detailed in Fig. 1. The pseudo-first-order kinetic plots of $\log(q_e\text{-}q_t)$ vs time showed a good linearity and a very low deviation between the calculated and the experimental q_e but the pseudo-second-order model is highly linear and fit extremely well, with correlation coefficients very close to 1 (0.9995 and 0.9996). It also showed very low deviation between the calculated and the experimental q_e. According to the pseudo-second-order model, the biosorption rate of Fe(II) is controlled by the adsorption on the internal surfaces of the pores of the plant powder. In this model, the rate-limiting step is the surface adsorption that involves chemisorption of Fe(II), in which removal is due to physicochemical interactions between the two phases (Robati 2013).

Biosorption studies of As(V)

Following the adsorption study of Fe(II) onto different biomaterials, the best candidate, *P. stratiotes* called Fe(II)-Ps from now on, was selected for investigating the adsorption of As(V). The study has been performed using aqueous solution of disodium hydrogen arsenate heptahydrate ($Na_2HAsO_4 \bullet 7H_2O$) at initial concentrations of 500 and 50 µg.L^{-1}, which have been found in contaminated areas (Salsignes, Aude, France) and corresponding to 50 and 5 times the standard for drinking water.

Optimization of the biosorption conditions of As(V)

Transformation of Fe(II)-Ps into Fe(III)-Ps

It is well known that in nature, arsenic oxyanions have strong affinities for iron(III) oxides (Grafe et al. 2001; Roberts et al. 2004). It would have been more convenient to directly load Fe(III) onto the biosorbent for the following biosorption of As(V). However, since Fe(III) does not well adsorb on biomaterials, the transformation of Fe(II)-Ps into Fe(III)-Ps was required and a thermal treatment was considered to perform this oxidation.

The influence of the thermal treatment of Fe(II)-Ps on the adsorption of As(V) was studied using different sets of activation temperature: 80, 150, 300 and 550 °C (Online Resource Tables 12 and 13). The biosorption capacity was clearly improved by increasing the temperature until reaching 550 °C. The highest temperature of 550 °C gave the best and remarkable biosorption capacity of 0.439 mg As(V) per gram biosorbent and 84% of As(V) was removed from the solution. This temperature was chosen as the thermal treatment for the rest of the study.

Concentration of Fe in Fe(III)-Ps

In order to provide the best biomaterial for arsenic removal, its concentration of Fe has been studied. Several biosorptions of Fe(II) were performed onto *P. stratiotes* with different concentrations of iron sulfate of 0, 5, 8 and 40 mg.L^{-1} and led to Fe(II)-Ps with iron content in weight % of 0.96, 3.4, 5.6 and 11.7, respectively. After a thermal treatment, the generated Fe(III)-Ps materials were compared for the biosorption of As(V) at 500 µg.L^{-1} (Online Resource Table 14).

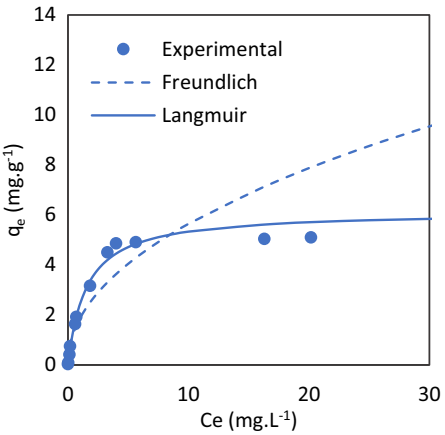

Isotherm	Parameters	As(V)
Freundlich	R^2	0.8759
	K_f (mg.g^{-1})	1.87
	n	2.12
Langmuir	R^2	0.9983
	q_m (mg.g^{-1})	6.11
	K_L (L.mg^{-1})	0.68
	R_L	0.04-0.23

Fig. 2 Freundlich and Langmuir adsorption isotherms and parameters for arsenate biosorption using Fe(III)-Ps

As expected, the adsorption performances of As(V) increase with the concentration of Fe(III) in the biosorbent. Fe(III)-Ps materials, enriched with at least 5 w% Fe, could lead to a final aqueous concentration of 84 µg.L^{-1} As(V), representing a good abatement of 83%. Interestingly, the concentration of Fe(II) in aqueous solution to realize such depollution of As(V) is relatively low and easy to find, as iron is abundant in the nature.

Comparative study between batch and fixed-bed adsorption modes

A comparison was made between the mode of adsorption, batch or column, at different concentrations of As(V). In the batch experiment, all the biosorbent is exposed to all the As(V) in solution during the entire experiment. Conversely, in the column experiment, each cm^3 of solution is exposed to the biosorbent during a fairly short period of time but is forced to go through the full length of the column (Online Resource Table 15). Although the two modes are very different in principle, they gave the same performances, offering flexibility in the technology to set up. This is an important aspect as both modes can be attractive in terms of potential scale-up. Both set-ups gave an excellent maximum capacity of biosorption of 5.1 mg.g^{-1} of As(V).

Adsorption isotherms of As(V)

The adsorption isotherm experiments of As(V) were conducted in batch mode by preparing solutions of $Na_2HAsO_4 \bullet 7H_2O$ with a concentration range of 0.5 to 20 mg.L^{-1} and using 1 g of Fe(III)-Ps per liter of solution. Experimental equilibrium data were fitted to the Langmuir and Freundlich adsorption isotherm models (Fig. 2 & Online Resource Fig. 13).

For the adsorption of As(V), the linearization with the Freundlich isotherm was not acceptable with an R^2 of 0.875, but the fitting with the Langmuir model was extremely good, with an R^2 of 0.998. The adsorption of As(V) onto Fe(III)-Ps appeared to be monolayered onto equal adsorption sites. The value of the Langmuir

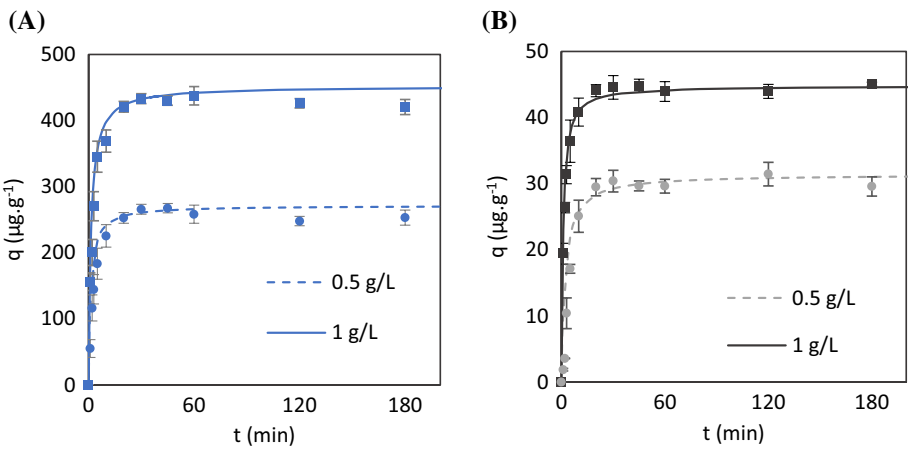

Fig. 3 Kinetic experimental data for As(V) biosorption onto Fe(III)-Ps and pseudo-second-order fitting; initial As concentration: 500 µg.L^{-1} (**A**) 50 µg.L^{-1} (**B**); dashed and full lines: 0.5 g.L^{-1}and 1 g.L^{-1} Fe(III)-Ps respectively

Table 2 BET analyses of Fe(III)-Ps and As(V)-Fe(III)-Ps biosorbents

	BET surface area (m^2/g)	Micropore volume (cm^3/g)	Micropore area (m^2/g)
Fe(III)-Ps	0.5762	0.003351	7.2444
As(V)-Fe(III)-Ps	18.5398	0.003517	6.6986

separation factors R_L (0.35–0.81) also revealed a favorable adsorption. The Langmuir modeling allowed the calculation of a theoretical maximum biosorption capacity of 6.14 $mg.g^{-1}$, which was almost reached experimentally by increasing the concentration of As(V), as noticed previously in the comparison of batch and column mode ("Comparative study between batch and fixed-bed adsorption modes" pp 13), and gave an experimental maximum capacity of As(V) biosorption of 5.1 $mg.g^{-1}$. This is a very good performance and competitive to what can be found in the literature, especially when comparing to other biomaterials. Indeed, other iron-enriched biosourced or natural materials, such as iron-coated sand (Kumar et al. 2008), iron-coated cellulose (Kumar et al. 2008), iron-coated cork granulate (Pintor et al. 2018), iron-coated wheat straw (Tian et al. 2011), iron-coated sawdust (Arshad and Imran 2020), iron-treated coconut shell (Emahi et al. 2019) and iron chitosan granules (Gupta et al. 2009), have been tested for removal of As(V) and gave a range of q_{max} of 1.6–8.1 $mg.g^{-1}$. Higher maximum biosorption capacities of As(V) were obtained with other materials, but the nature, abundance and mode of preparation of the materials used in adsorption should be considered in addition to the biosorption performances.

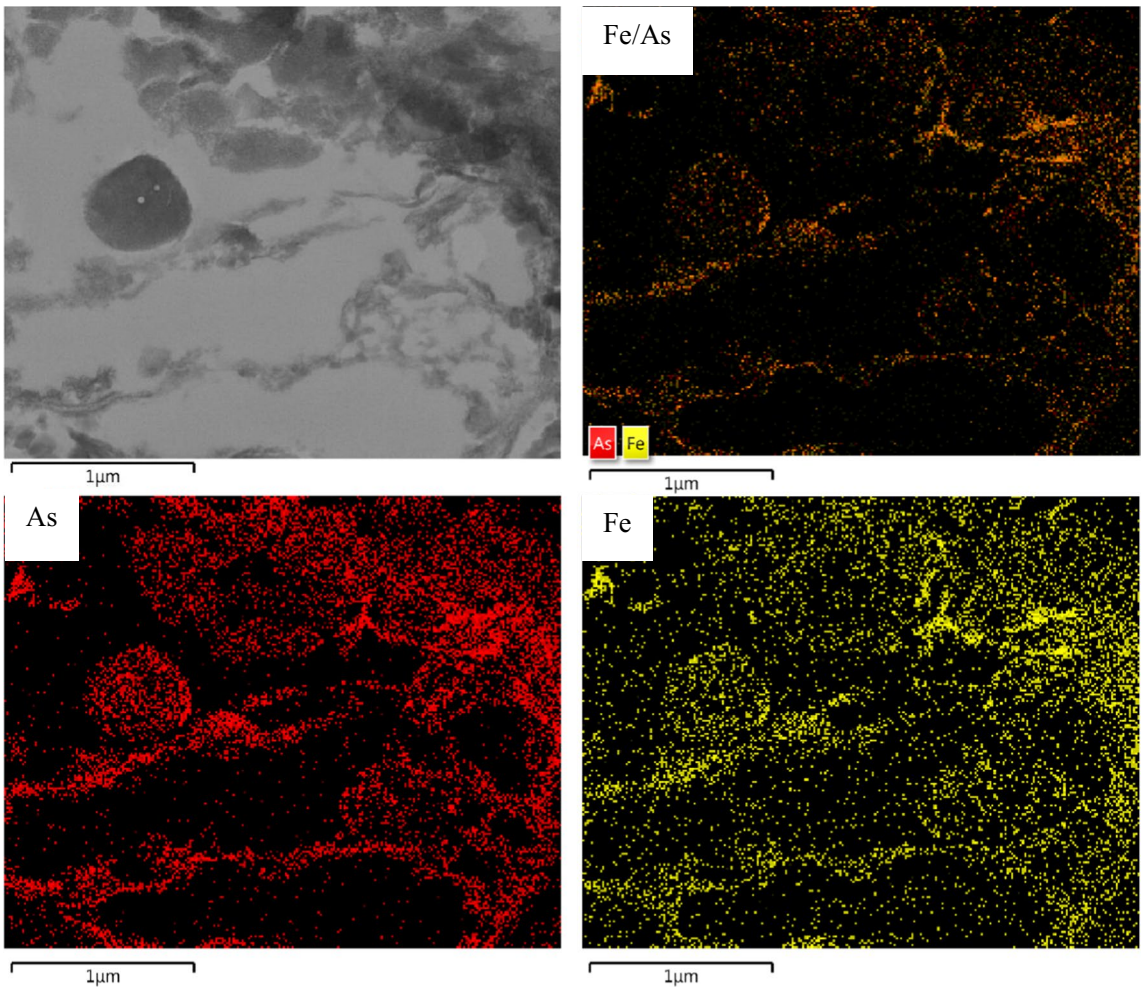

Fig. 4 Scanning transmission electron microscopy of As(V)-Fe(III)-Ps

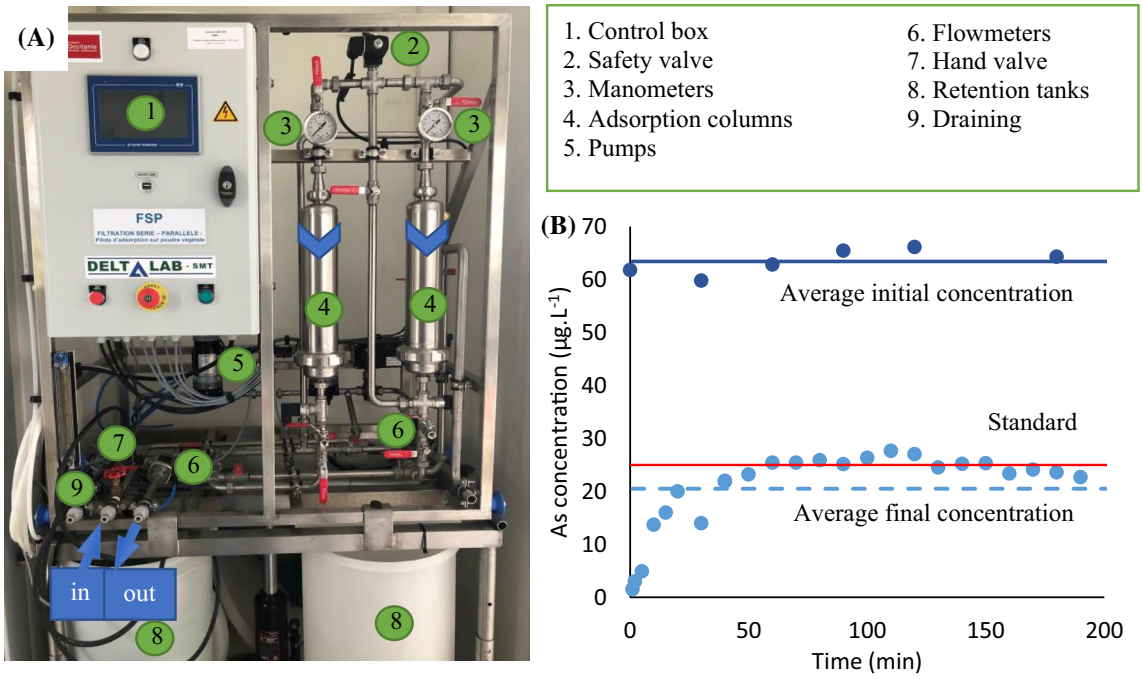

Fig. 5 **A** Photograph of the pilot; **B** monitoring of As(V) removal from the Russec river

Adsorption kinetics of As(V)

The adsorption behavior kinetics of As(V) was studied with concentrations of 50 and 500 µg.L^{-1} of $Na_2HAsO_4 \bullet 7H_2O$ using 0.5 and 1 g of Fe(III)-Ps. In each case, the biosorption of As(V) was very rapid and reached the equilibrium in only 30 min (Fig. 3). The profiles are very similar to the biosorption of Fe(II) discussed previously: a first step corresponding to rapid filling of the adsorption sites during the first 30 min, followed by a slower step with no significant increase in arsenate uptake.

It is interesting to notice that the equilibrium is reached at the same time using 0.5 or 1 g.L^{-1} of biosorbent, but with a different arsenic removal, 60% or 80%, respectively. This equilibrium is reached when no more adsorption sites are available either because they are occupied or because of repulsion forces avoiding their accessibility.

Additionally the kinetics is the same with 50 or 500 µg.L^{-1} of As(V).

For each configuration studied, the adsorption of As(V) onto Fe(III)-Ps is best described by the pseudo-second-order kinetic model as illustrated by the linearization and the correlation coefficients (Online Resource Fig. 14 and Table S18, $R^2 > 0.99$). According to the pseudo-second-order model, the biosorption is based on the sorption capacity of the solid phase and controlled by chemosorption (Ho and McKay 1998).

Characterization of biosorbents

BET analyses of Fe(III)-Ps and As(V)-Fe(III)-Ps The morphologies of Fe(III)-Ps and As(V)-Fe(III)-Ps have been determined by BET analyses (Table 2). The biomaterial of Fe(III)-Ps shows a low BET surface area and a low porosity. The morphology of the Fe(III)-Ps biomaterial cannot explain the efficiency of As(V) biosorption, suggesting that Fe(III) sorbs As(V).

XRPD analyses of Fe(III)-Ps and As(V)-Fe(III)-Ps XRPD analyses were performed on Fe(III)-Ps and on As(V)-Fe(III)-Ps (Online Resource Fig. 18). However, XRPD analyses only showed calcium carbonate crystals, as ferrous complexes rarely give crystals.

HRTEM/EDX and Mössbauer analyses of As(V)-Fe(III)-Ps HRTEM coupled with EDX analyses have been performed on the Fe(III)-Ps biomaterial after biosorption of As(V). The TEM images and EDX spectra clearly show that the dispersion of these two elements is linked to each other (Fig. 4 and Online Resource Fig. 15). Indeed, As is co-

localized with Fe but Fe is not systematically present where As is. In other words, As is not present if Fe is absent. This observation suggests that Fe cations interact with As oxyanions forming mixed As/Fe complexes.

Mössbauer spectroscopy was performed to characterize the interaction between Fe(III) and As(V) (Online Resource Fig. 17). Mössbauer spectrum of the Fe(III)-Ps biomaterial suggests the unique presence of Fe(O)OH species, as IS and EQ values similar to the iron(III) oxide-hydroxide mineral, called akaganeite (Online Resource Table 21). Mössbauer spectrum of As(V)-Fe(III)-Ps only shows a decrease in intensity of the quadrupole splitting, but no other signal. It suggests an interaction between Fe(III) and As(V) in which Fe becomes another species but in too small quantities to be detected.

FTIR analyses of root powder of *Pistia stratiotes*, Fe(II)-Ps, Fe(III)-Ps and As(V)-Fe(III)-Ps Infrared analyses were performed to deepen the mechanism of adsorption of Fe(II) and As(V) onto the biosorbents. FTIR analyses of the root powder of *P. stratiotes* and Fe(II)-Ps, post-adsorption of Fe(II), were first compared. Deconvoluted FTIR spectrum of *P. stratiotes* shows a band at 1640 cm^{-1} corresponding to the stretching vibration of free carboxylate moieties (Online Resource Fig. 19A). After adsorption of Fe(II), deconvoluted FTIR spectrum of Fe(II)-Ps shows a blue shift of carboxylate band at 1625 cm^{-1}, suggesting the interaction between the carboxylate moieties and Fe(II) (Online Resource Fig. 19B).

FTIR analyses of Fe(III)-Ps and As(V)-Fe(III)-Ps, post-adsorption of As(V), were then compared to explore the adsorption mechanism of As(V) (Online Resource Fig. 20). Both spectra remain similar, with a large band at 1400 cm^{-1} corresponding to calcium carbonate, but a band at 1150 cm^{-1} clearly disappeared on As(V)-Fe(III)-Ps. This observation shows that the presence of As(V) modifies sites of Fe(O)OH on the biomaterial via an interaction, but the nature of the interaction remains difficult to define.

As(V) removal from the polluted Russec river (Orbiel valley, Occitanie, France)

Our two-step methodology has been tested to remove As(V) from wastewater that was collected in Aude region of France in the Russec river, which is polluted by arsenic. Prior to biosorption, a speciation analysis of the water from Russec river has been carried out by separation onto anionic column (PRP-X100) and quantification by ICP-MS and could show that, as expected from a surface water, 96.9% of the arsenic is under its oxidized form As(V) (Online Resource Table 19).

A pilot decontamination apparatus has been engineered for this study (Fig. 5 and Online Resource paragraph 1.4). It is a mobile unit, whose characteristics have been chosen to make it usable in different specific cases. This filtration device is constituted of two adsorption columns (1 L), usable in series or in parallel, allowing the removal of different metallic pollutants according to the filtrating media charged inside. A pump allows the circulation of the polluted effluent, up to 200 $L.h^{-1}$ and 10 bar, through the columns (inlet and outlet retention tank of 50 L). Sensors measure pressure and flow rate, and a control box allows the regulation of the pump, flowrate and pressure with real-time display, and collect the data.

This pilot has been tested on site using 100 g of the Fe(III)-Ps biosorbent and pumping water from Russec river at 30 $L.h^{-1}$ for 3 h. Samples were collected every 10 min and analyzed by GF-AAS (Fig. 5 and Online Resource Table 20). The results are very encouraging as the pilot could remove 67% of As(V) from the wastewater and reached below the European standard for industrial effluents of 25 $\mu g.L^{-1}$ (NOR: ATEP9870017A 2020) (NOR: ATEP9870017A—consolidated on the 31 December 2020 https://www.legifrance.gouv.fr/loda/id/LEGITEXT000005625281/ s. d.). In this experiment, 90 L of wastewater has been decontaminated and the biosorbent was not saturated after 3 h and could be used longer.

Conclusion

A two-step biosorption methodology was developed for removing arsenic from aqueous synthetic solutions and mining effluents, using bio-wastes firstly enriched with iron by a prior biosorption. This innovative technique allowed several environmental services as a double, rapid and efficient decontamination of As and Fe based on simple operations using low-cost invasive alien species as biosorbents and that follows mathematical models remarkably well, with a good repeatability. The robustness of this methodology could be adapted for the development of a pilot plan, which was tested and validated *in natura*.

This result reveals that these natural and low-cost materials can follow mathematical models remarkably well, with good repeatability, and proves the robustness of the method.

Acknowledgements The authors would like to thank the French National Center for Scientific Research (CNRS) for financial support. Sci-GuidEdit is acknowledged for writing assistance and proof-reading the article. Sébastien Diliberto is acknowledged for Mossbauer spectroscopy assessments.

Author contributions C.G. has conceived and designed the study. K.R., A.G. and Y.-M. L. carried out the harvest, preparation of samples and analyses. C.G. and K.R. completed integrated data analyses and wrote the paper.

Availability of data and materials The data that support the findings of this study are available from the supporting materials.

Declarations

Ethics approval and consent to participate Not applicable.

Consent for publication Not applicable.

Conflict of interest The authors declare no conflict of interest.

References

Arshad N, Imran S (2020) Indigenous waste plant materials: an easy and cost-effective approach for the removal of heavy metals from water. Curr Res Green Sustain Chem 3:100040. https://doi.org/10.1016/j.crgsc.2020.100040

Carlson L, Bigham JM, Schwertmann U, Kyek A, Wagner F (2002) Scavenging of As from acid mine drainage by schwertmannite and ferrihydrite: a comparison with synthetic analogues. Environ Sci Technol 36(8):1712–1719. https://doi.org/10.1021/es0110271

Choudhary M, Bhattacharyya KG (2020) As(III) and As(V) remediation in an aqueous medium using a cellulosic biosorbent: kinetics, equilibrium, and thermodynamics study. SN Appl Sci 2(10):1653. https://doi.org/10.1007/s42452-020-03426-2

Emahi I, Sakyi PO, Bruce-Vanderpuije P, Issifu AR (2019) Effectiveness of raw versus activated coconut shells for removing arsenic and mercury from water. Environ Nat Resour Res 9(3):127. https://doi.org/10.5539/enrr.v9n3p127

Fan L, Zhang S, Zhang X, Zhou H, Zexiang L, Wang S (2015) Removal of arsenic from simulation wastewater using nano-iron/oyster shell composites. J Environ Manag 156:109–114. https://doi.org/10.1016/j.jenvman.2015.03.044

Grafe M, Eick MJ, Grossl PR (2001) Adsorption of Arsenate (V) and Arsenite (III) on goethite in the presence and absence of dissolved organic carbon. Soil Sci Soc Am J 65(6):1680–1687. https://doi.org/10.2136/sssaj2001.1680

Gupta A, Chauhan VS, Sankararamakrishnan N (2009) Preparation and evaluation of iron-chitosan composites for removal of As(III) and As(V) from arsenic contaminated real life groundwater. Water Res 43(15):3862–3870. https://doi.org/10.1016/j.watres.2009.05.040

Gupta A, Vidyarthi SR, Sankararamakrishnan N (2015) Concurrent removal of As(III) and As(V) using green low Cost functionalized biosorbent—saccharum officinarum bagasse. J Environ Chem Eng 3(1):113–121. https://doi.org/10.1016/j.jece.2014.11.023

Hao L, Zheng T, Jiang J, Qi Hu, Li X, Wang P (2015) Removal of As(III) from water using modified jute fibres as a hybrid adsorbent. RSC Adv 5(14):10723–10732. https://doi.org/10.1039/C4RA11901K

Ho YS, McKay G (1998) A comparison of chemisorption kinetic models applied to pollutant removal on Various Sorbents. Process Saf. Environ. Prot. 76:332–340. https://doi.org/10.1205/095758298529696

Ho YS, McKay G (1999) Pseudo-second order model for sorption processes. Process Biochem 34(5):451–465. https://doi.org/10.1016/S0032-9592(98)00112-5

Hu G, Huang S, Chen H, Wang F (2010) Binding of four heavy metals to hemicelluloses from rice bran. Food Res Int 43(1):203–206. https://doi.org/10.1016/j.foodres.2009.09.029

Irshad S, Xie Z, Mehmood S, Nawaz A, Ditta A, Mahmood Q (2021) Insights into conventional and recent technologies for arsenic bioremediation: a systematic review. Environ Sci Pollut Res 28(15):18870–18892. https://doi.org/10.1007/s11356-021-12487-8

Kumar A, Gurian PL, Bucciarelli-Tieger RH, Mitchell-Blackwood J (2008) Iron oxide-coated fibrous sorbents for arsenic removal. J Am Water Works Assoc 100(4):151-A4. https://doi.org/10.1002/j.1551-8833.2008.tb09611.x

Mohan D, Pittman CU (2007) Arsenic removal from water/wastewater using adsorbents—a critical review. J Hazard Mater 142(1–2):1–53. https://doi.org/10.1016/j.jhazmat.2007.01.006

Monrad M, Ersbøll AK, Sørensen M, Baastrup R, Hansen B, Gammelmark A, Tjønneland A, Overvad K, Raaschou-Nielsen O (2017) Low-level arsenic in drinking water and risk of incident myocardial infarction: a cohort study. Environ Res 154:318–24. https://doi.org/10.1016/j.envres.2017.01.028

NOR: ATEP9870017A—consolidated on the 31 December 2020. https://www.legifrance.gouv.fr/loda/id/LEGITEXT000005625281/.

Pehlivan E, Tran HT, Ouédraogo WKI, Schmidt C, Zachmann D, Bahadir M (2013) Sugarcane bagasse treated with hydrous ferric oxide as a potential adsorbent for the removal of As(V) from aqueous solutions. Food Chem 138(1):133–38. https://doi.org/10.1016/j.foodchem.2012.09.110

Pintor AMA, Vieira BRC, Santos SCR, Boaventura RAR, Botelho CMS (2018) Arsenate and arsenite adsorption onto iron-coated cork granulates. Sci Total Environ 642:1075–89. https://doi.org/10.1016/j.scitotenv.2018.06.170

Robati D (2013) Pseudo-second-order kinetic equations for modeling adsorption systems for removal of lead ions using multi-walled carbon nanotube. J Nanostructure Chem 3(1):55. https://doi.org/10.1186/2193-8865-3-55

Roberts LC, Hug SJ, Thomas Ruettimann Md, Billah M, Khan AW, Rahman MT (2004) Arsenic removal with Iron(II) and Iron(III) in waters with high silicate and phosphate concentrations. Environ Sci Technol 38(1):307–15. https://doi.org/10.1021/es0343205

Sarkar A, Paul B (2016) The global menace of arsenic and its conventional remediation—a critical review. Chemosphere 158:37–49. https://doi.org/10.1016/j.chemosphere.2016.05.043

Setyono D, Valiyaveettil S (2014) Chemically modified sawdust as renewable adsorbent for arsenic removal from water. ACS Sustain Chem Eng 2(12):2722–29. https://doi.org/10.1021/sc500458x

Stanovych A, Balloy M, Olszewski TK, Petit E, Grison C (2019) Depollution of mining effluents: innovative mobilization of plant resources. Environ Sci Pollut Res 26(19):19327–34. https://doi.org/10.1007/s11356-019-05027-y

Sudipta G, Debsarkar A, Dutta A (2019) Technology alternatives for decontamination of arsenic-rich groundwater—a critical review. Environ Technol Innov 13:277–303. https://doi.org/10.1016/j.eti.2018.12.003

Tian Y, Min W, Lin X, Huang P, Huang Y (2011) Synthesis of magnetic wheat straw for arsenic adsorption. J Hazard Mater 193:10–16. https://doi.org/10.1016/j.jhazmat.2011.04.093

United Nations World Water Development Report 2021: Valuing Water (2021) S.l.: United Nations Educational, Scientific and Cultural Organization. https://unesdoc.unesco.org/ark:/48223/pf0000375724

Williams M (2001) Arsenic in mine waters: an international study. Environ Geol 40(3):267–78. https://doi.org/10.1007/s002540000162